Atmospheric Environment 109 (2015) 70–78

Contents lists available at ScienceDirect

Atmospheric Environment

journal homepage: www.elsevier.com/locate/atmosenv

Use of isotopic compositions of nitrate in TSP to identify sources and chemistry in South China Sea

Hong-Wei Xiao [a, *], Lu-Hua Xie [b], Ai-Min Long [a], Feng Ye [b], Yue-Peng Pan [c], Da-Ning Li [d], Zhen-Hua Long [d], Lin Chen [d], Hua-Yun Xiao [e, *], Cong-Qiang Liu [e]

[a] State Key Laboratory of Tropical Oceanography, South China Sea Institute of Oceanology, Chinese Academy of Sciences, Guangzhou 510301, China
[b] Key Laboratory of Marginal Sea Geology, Guangzhou Institute of Geochemistry, Chinese Academy of Sciences, Guangzhou 510640, China
[c] State Key Laboratory of Atmospheric Boundary Layer Physics and Atmospheric Chemistry, Institute of Atmospheric Physics, Chinese Academy of Sciences, Beijing 100029, China
[d] Xisha Deep Sea Marine Environment Observation and Research Station, South China Sea Institute of Oceanology, Chinese Academy of Sciences, Sansha 157009, China
[e] State Key Laboratory of Environmental Geochemistry, Institute of Geochemistry, Chinese Academy of Sciences, Guiyang 550002, China

HIGHLIGHTS

- $\delta^{15}N$ and $\delta^{18}O$ of NO_3^- were observed in oligotrophic South China Sea.
- NO_x is major from anthropogenic sources of southern China in cool months.
- Decrease in $\delta^{15}N$ and increase in $\delta^{18}O$ during transport from coast to remote marine.
- 47.9% of NO_3^- is from NO_x conversion in South China Sea during transport.

ARTICLE INFO

Article history:
Received 11 September 2014
Received in revised form
2 March 2015
Accepted 5 March 2015
Available online 6 March 2015

Keywords:
Nitrogen isotope
Oxygen isotope
South China Sea
Nitrate
Atmospheric chemical process
Isotopic fractionation

ABSTRACT

NO_3^- concentration, nitrogen and oxygen isotopic compositions ($\delta^{15}N$ and $\delta^{18}O$) of NO_3^- were measured in total suspended particulates (TSP) at Yongxing Island in the South China Sea (SCS) between Feb. 2013 and Jan. 2014, as well as on two cruises in the northern South China Sea (NSCS). Measurements aimed to identify NO_3^- sources, and possible chemical formation processes of NO_3^-. The $\delta^{15}N$ and $\delta^{18}O$ of NO_3^- in TSP at Yongxing Island ranged from −2.5 to +4.9‰, and +48.1 to +99.0‰, with annual weighted averages of +1.5‰ and +83.2‰, respectively. Both $\delta^{15}N$ and $\delta^{18}O$ had higher values in cool months, indicating that NO_x sources and oxidants were different between seasons. In cool months, NO_x was mainly from anthropogenic sources, particularly from coal combustion in South China, resulting in high nitrogen deposition that was oxidized by O_3 to NO_3^-. In warm months, natural emissions were an important source of NO_x. TSP samples in the NSCS had higher NO_3^- concentrations, higher $\delta^{15}N$ and lower $\delta^{18}O$ values than samples from Yongxing Island over the same period. This suggests that atmospheric processes caused a decrease in NO_3^- concentrations and $\delta^{15}N$ but increase in $\delta^{18}O$ from coast to remote marine. Assuming to oxygen atoms were derived from O_3 during transport in cool months, the mean ratio of NO_3^- formed by NO_x to total NO_3^- was calculated to be 47.9%. This suggests the mean loss ratio of NO_x was 89% while the loss ratio of NO_3^- was 87% during transport between Chinese coastal areas and Yongxing Island in Nov., 2013.

1. Introduction

Nitrogen is an essential element for growth and reproduction in both plants and animals in terrestrial and marine ecosystems. Most nitrogen is present as N_2, comprising about 80% of the atmosphere, which is available only to diazotrophs (Duce et al., 2008). Most life can only use reactive nitrogen species (NO_x, NH_y, and organic

* Corresponding authors.
E-mail addresses: xiaohw@scsio.ac.cn (H.-W. Xiao), xiaohuayun@vip.skleg.cn (H.-Y. Xiao).

http://dx.doi.org/10.1016/j.atmosenv.2015.03.006
1352-2310/

nitrogen) (Kim et al., 2014). In most parts of the open ocean, concentrations of bio-available nitrogen limit primary production, which largely controls the efficiency of the 'biological pump' (Falkowski et al., 1998). One of major input pathways of new reactive nitrogen to the ocean is through atmospheric deposition, accounting for about 30% of new reactive nitrogen input (Duce et al., 2008). Global atmospheric nitrogen deposition has increased markedly over the last 100 years, and about 67 Tg of atmospheric-derived reactive nitrogen inputs into the global ocean every year, mainly owing to human activities (Duce et al., 2008; Hastings et al., 2009). Thus, about 50% of anthropogenic reactive nitrogen in the atmosphere is deposited to the ocean (Duce et al., 2008; Kim et al., 2014).

NO_x (NO and NO_2) is a major component of atmospheric reactive nitrogen and is a precursor of NO_3^- (Altieri et al., 2013; Galloway et al., 2008; Olivier et al., 1998; Yang et al., 2014). NO_x is mainly from combustion of fossil fuel, lightning, biomass burning and soil processes (Davidson and Kingerlee, 1997; Hsu et al., 2014; Finlayson-Pitts and Pitts Jr, 1999; Morin et al., 2009; Schumann and Huntrieser, 2007). Nitrate (NO_3^-), as the main nitrogen species involved in atmospheric deposition, is formed from oxidation of NO_x through several chemical pathways (Altieri et al., 2013; Chameides, 1984; Finlayson-Pitts and Pitts Jr, 1999; Morin et al., 2009; Seinfeld and Pandis, 2012). In general, NO is in photochemical equilibrium with NO_2 (R1 and R2), then NO_2 is oxidized to HNO_3 by the hydroxyl (OH) radical during the day (R3), and by ozone (O_3) to form the NO_3 radical (R4), which subsequently combines with NO_2 to form N_2O_5 (R5), and then undergoes hydrolysis to form HNO_3 (R7) over night (Altieri et al., 2013; Fang et al., 2011). In reaction R5, NO_2 and NO_3 have a thermal equilibrium reaction with N_2O_5. NO_3 also reacts with volatile organic compounds, including dimethyl sulfide (DMS) (R6) (Altieri et al., 2013; Gobel et al., 2013). OH pathways are more prevalent in the summer than in the winter, but N_2O_5 pathways are more important than OH pathways in winter (Altieri et al., 2013; Calvert et al., 1985). These major oxidation pathways are shown in Supplementary Text S1.

Nitrogen and oxygen isotopic compositions ($\delta^{15}N$ and $\delta^{18}O$) are usually used to distinguish nitrate sources and the chemical formation processes in the atmosphere (Altieri et al., 2013; Elliott et al., 2009; Gobel et al., 2013; Hastings et al., 2003; Morin et al., 2009; Yang et al., 2014). Values of $\delta^{15}N$ of atmospheric NO_3^- are often used to identify NO_x sources, because most NO_x is converted to NO_3^- through atmospheric reactions (Elliott et al., 2009; Heaton, 1987; Moore, 1977; Xiao and Liu, 2002; Xiao et al., 2012). Different NO_x sources have different nitrogen isotopic composition, including vehicle fuel combustion, coal combustion, diesel combustion, natural gas combustion, lightning, livestock and biogenic soil emissions, shown as in Fig. S1 (Ammann et al., 1999; Felix et al., 2012; Felix and Elliott, 2014; Fibiger et al., 2014; Hastings et al., 2009; Heaton, 1990; Hoering, 1957; Kiga et al., 2000; Li and Wang, 2008; Moore, 1977). Direct measurements values of $\delta^{15}N$ of NO_x from biomass burning are not reported, but previous studies of NO_3^- in pre-industrial ice suggest that natural sources of NO_x have positive $\delta^{15}N$ source signatures (Freyer, 1996; Hastings et al., 2009). In contrast, $\delta^{18}O$ values change very much during conversion of NO_x to NO_3^- because oxygen atoms in NO_x are exchanged rapidly with O_3 (R1 and R2). Then, NO_3^- is formed through multiple pathways, including but not limited to N_2O_5 and OH pathways. These pathways are influenced by many factors, e.g., weather conditions, and the availability of reactive aerosol surfaces (Wankel et al., 2010). Typically, $\delta^{18}O{-}O_3$ ranges from +90 to +122‰, while the $\delta^{18}O{-}OH$ radical ranges from −15 to 0‰ over Asia (Fang et al., 2011; Johnston and Thiemens, 1997; Krankowsky et al., 1995).

In this study, nitrate concentrations, and $\delta^{15}N$ and $\delta^{18}O$ of nitrate in TSP at Yongxing Island and on two cruises in the NSCS were measured to investigate nitrate sources. We also use these data to provide insights into the chemical pathways involving conversion of NO_x to NO_3^- in this region.

2. Methods

Total suspended particulates (TSP) were sampled at Yongxing Island (16.83°N, 112.33°E) between Feb. 28, 2013 and Jan. 17, 2014 and on two cruises of the Research Vessel "Shiyan 3", in the NSCS, over two periods from 6 to 16 Aug. 2012 and from 4 Nov. to 6 Dec. 2013, (Fig. S2 and Table S1). TSP samples were collected using a special high-flow rate (1.05 ± 0.03 m^3/min) KC-1000 sampler (see supplementary text S2).

The concentrations of NO_2^- and NO_3^- in TSP samples were determined using the Dionex ICS-90 Ion Chromatography System (Dionex Corporation, California, USA). The $\delta^{15}N$ and $\delta^{18}O$ values of NO_3^- were measured using the Cd-reduction method (see supplementary text S2; McIlvin and Altabet, 2005; Ryabenko et al., 2009).

To determine the sources of TSP, air mass back trajectories and a concentration weighted trajectory (CWT) for nitrate were computed using TrajStat software (Wang et al., 2009; see supplementary text S3).

3. Results

3.1. Nitrate concentrations in TSP

Concentrations of TSP ranged from 11.8 to 117.4 μg/m^3, with an average concentration of 58.1 ± 20.6 μg/m^3 at Yongxing Island between Feb., 2013 and Jan., 2014 (Table 1). The TSP values show no significant correlations with temperature, relative humidity, or rainfall amount, but are correlated with wind speed ($R = 0.65$, $P < 0.001$). There is a strong sinusoidal relationship between TSP concentrations and month ($R = 0.91$, $P = 0.0048$), with higher values in winter and lower ones in summer. NO_3^- concentrations ranged from 4.9 to 103.8 nmol/m^3, with an average concentration of 34.9 ± 12.1 nmol/m^3. In the warm months (May to Aug.), average NO_3^- concentration was 27.3 nmol/m^3, much lower than that for cooler months (45.1 nmol/m^3, Mar. 2013, Oct. 2013 to Jan. 2014). However, there were no significant correlations between NO_3^- concentration and month ($P > 0.05$).

Table 1
Concentrations of TSP, NO_3^-, $\delta^{15}N$ and $\delta^{18}O$ of NO_3^- in TSP at Yongxing Island and on two cruises in Northern South China Sea.

Location	Month	TSP (μg/m^3)	NO_3^- (nmol/m^3)	$\delta^{15}N$ (‰)[a]	$\delta^{18}O$ (‰)[a]
Yongxing Island	2013.03	30.4 ± 17.5	35.9 ± 9.5	+(2.4 ± 0.9)	+(83.1 ± 7.8)
	2013.04	37.5 ± 15.8	34.7 ± 11.5	+(2.4 ± 1.0)	+(86.1 ± 7.7)
	2013.05	46.2 ± 27.8	32.2 ± 8.2	-(0.6 ± 1.5)	+(72.6 ± 1.3)
	2013.06	42.0 ± 32.5	24.5 ± 13.7	-(0.1 ± 0.9)	+(75.1 ± 4.1)
	2013.07	43.5 ± 27.2	19.9 ± 10.6	(0 ± 1.6)	+(67.1 ± 7.6)
	2013.08	68.4	32.5	+(0.9 ± 0.6)	+(58.9 ± 4.9)
	2013.09	45.7 ± 35.8	21.6 ± 15.2	+(1.4 ± 0.8)	+(72.4 ± 3.8)
	2013.10	82.7 ± 28.5	52.8 ± 33.7	+(2.4 ± 1.4)	+(87.8 ± 4.4)
	2013.11	79.5 ± 31.4	37.5 ± 21.8	+(1.8 ± 0.9)	+(88.6 ± 6.4)
	2013.12	78.0 ± 3.9	59.2 ± 15.5	+(2.0 ± 0.6)	+(92.8 ± 1.9)
	2014.01	85.1 ± 5.0	40.2 ± 8.8	+(0.3 ± 0.4)	+(94.2 ± 2.4)
	Average	58.1 ± 20.6	34.9 ± 12.1	+(1.5 ± 1.6)	+(83.2 ± 10.6)
Northern[b] South China Sea	2012.08	101.8 ± 47.3	113.5 ± 84.9	+(4.9 ± 6.4)	+(65.6 ± 12.1)
	2013.11	104.3 ± 24.7	130.6 ± 54.7	+(5.4 ± 0.9)	+(71.8 ± 9.2)

[a] Weighted average by the amount of nitrate with standard deviation.
[b] See the Table S1 for more information about data.

In samples collected on the two cruises in the NSCS, average concentrations of TSP were 101.8 ± 47.3 μg/m^3 in Aug. 2012 and 104.3 ± 24.7 μg/m^3 in Nov. 2013 (Table 1), showing that there were no significant changes between warm (Aug. 2012) and cool (Nov. 2013) months in the NSCS. However, atmospheric aerosol concentrations in the remote ocean were much lower than that for coastal regions. Likewise, the average concentrations of NO_3^- in the NSCS were 113.5 ± 84.9 nmol/m^3 in Aug. 2012 and 130.6 ± 54.7 nmol/m^3 in Nov. 2013. Differences in NO_3^- concentrations between warm and cool months were also observed in the SCS on two cruises reported in Hsu et al. (2014).

3.2. $\delta^{15}N$–NO_3^- in TSP

At Yongxing Island, $\delta^{15}N$–NO_3^- in TSP varied between −2.5 and +4.9‰, with an annual weighted average (by NO_3^- concentrations) of +1.5‰ (Table 1). In warm months, $\delta^{15}N$–NO_3^- in TSP ranged from −2.5‰ to +4.8‰, with a weighted average (by NO_3^- concentrations) of −0.3‰. While in cool months, it ranged from −0.1‰ to +4.9‰, with a weighted average (by NO_3^- concentrations) of +2.1‰. There were no significant correlations between $\delta^{15}N$ and NO_3^- ($P > 0.05$). Values of $\delta^{15}N$ exhibited sinusoidal variation with months ($y = 1.1 + 1.4\sin(2\pi x/8.0 + 0.5)$; $R = 0.89$, $P = 0.009$), with lowest values during the southwest monsoon (warm seasons) and highest values during the northeast monsoon (cool seasons). The average $\delta^{15}N$ value also was lower in Aug. 2012 than in Nov. 2013 in the NSCS (Table 1). The differences in $\delta^{15}N$ values between Yongxing Island and the NSCS for the same months were −4.0‰ in Aug. and −3.6‰ in Nov., indicating that the $\delta^{15}N$ value decreased from the NSCS to Yongxing Island.

3.3. $\delta^{18}O$–NO_3^- in TSP

The $\delta^{18}O$–NO_3^- in TSP samples values ranged from +48.1 to +99.0‰, with a weighted average value (by NO_3^- concentrations) of +83.2‰ at Yongxing Island, consistent with previous data (Altieri et al., 2013; Fang et al., 2011; Hastings et al., 2003; Morin et al., 2009; Yang et al., 2014). There was a significant correlation between $\delta^{18}O$ and NO_3^- ($P < 0.0001$, $R = 0.57$). Values of $\delta^{18}O$ also exhibited sinusoidal variation with months ($y = 77.5 + 13.2\sin(2\pi x/8.7 + 6.3)$, $R = 0.88$, $P = 0.01$). During warm months, the average value was +71.2‰; while during cool months, it was +88.9‰. In the NSCS, the values of $\delta^{18}O$ were +65.6‰ in Aug. 2012 and 71.8‰ in Nov. 2013, respectively. The differences in $\delta^{18}O$ values between Yongxing Island and NSCS were +6.7‰ in Aug. and −16.8‰ in Nov., respectively.

4. Discussions

4.1. Backward trajectories and concentration weighted trajectory

Backward trajectories indicate that almost all air masses were originated from northeast of Yongxing Island during the cool months (from Oct. to Mar.), or from southwest of the island during the warm months (from May to Aug.), as shown in Fig. S3a. But during transition months (Apr. and Sep.), air masses originated from the regions of northeast and southwest of the island (Fig. S3b). Backward trajectories calculated for the summer cruise in the NSCS, showed air masses were from the southwest quadrant of the SCS; while during winter cruise, they were from northeastern quadrant. These results are consistent with the backward trajectories calculated for Yongxing Island.

The CWT method applied to NO_3^- in TSP samples clearly shows that high concentrations came from developed coastal regions of China, with large anthropogenic emissions (Fig. 1). For instance, the NO_3^- was 228.9 nmol/m^3 at Shanghai (Wang et al., 2006), 96.8 nmol/m^3 at Taichung (Fang et al., 2002) and 154.7 nmol/m^3 at Guangzhou (Wang et al., 1992). Relatively lower concentrations were from Southeast Asia or locally in the SCS. These regions both have low emissions of NO_x, with values such as 19.4 nmol/m^3 at Phnom Penh, 17.6 nmol/m^3 at Serpong, 17.9 nmol/m^3 at Petaling Jaya, 2.84 nmol/m^3 at Tanah Rata, 1.28 nmol/m^3 at Danum Valley, 3.02 nmol/m^3 at Mt. Sto. Tomas, respectively (EANET sites; http://www.eanet.asia/).

4.2. Temporal and spatial variation in $\delta^{15}N$

The $\delta^{15}N$ of NO_3^- in TSP samples at Yongxing Island ranged from −2.5‰ to +4.9‰ from Feb. 2013 to Jan 2014, with a weighted average (by NO_3^- concentrations) of +1.5‰. The $\delta^{15}N$ of NO_3^- in TSP samples from the two cruises varied between −7.7‰ and +10.9‰ in Aug., with a weighted average (by NO_3^- concentrations) of +4.9‰; while in Nov., they were between +3.7‰ and +6.7‰, with a weighted average (by NO_3^- concentrations) of +5.4‰. All of the $\delta^{15}N$ values were within the previously reported ranges of $\delta^{15}N$ from NO_3^- (Elliott et al., 2009; Fang et al., 2011; Hastings et al., 2003; Heaton et al., 2004; Kendall, 1998; Morin et al., 2009; Savarino et al., 2007; Yang et al., 2014). The $\delta^{15}N$ average at Yongxing Island was lower than for both NSCS cruises. In addition, the $\delta^{15}N$ average for precipitation in urban and rural sites of Guangdong Province, near to the NSCS, also were higher than for NO_3^- in TSP at Yongxing Island, but close to values for NSCS TSP samples (Fang et al., 2011). In contrast, much lower values were found in aerosols from weddell Sea (Antarctic), Ny-Alesund (Arctic) and over the Altantic Ocean (Morin et al., 2009).

Seasonal variation in $\delta^{15}N$ in the atmosphere has been reported in many previous studies (Altieri et al., 2013; Elliott et al., 2009; Fang et al., 2011; Morin et al., 2008; Wankel et al., 2010). However the seasonal variation pattern observed in this study was different. The $\delta^{15}N$ values exhibited a sinusoidal variation with months at Yongxing Island, with higher values in cool months and lower values in warm months (Fig. 2a and b). This is contrary to the seasonal pattern observed in other studies (Altieri et al., 2013; Hastings et al., 2003; Wankel et al., 2010), and may be explained by differences in TSP sources.

Samples with backward trajectories from northeast of Yongxing Island during cool months, had higher NO_3^- concentrations and $\delta^{15}N$ values than samples with trajectories from southwest of Yongxing Island during warm months (Figs. 1 and 2). In the Pearl River Delta region, and east China, NO_x emissions are high (Zhang et al., 2007; Zheng et al., 2009), with >70% of NO_x emission from coal combustion (Tian et al., 2001). Thus, the higher NO_3^- concentrations and $\delta^{15}N$ values during cool months indicate an anthropogenic NO_x source, mainly from coal combustion (Fang et al., 2011). In contrast, most air masses originate from south of Yongxing Island during warm months (Fig. 2b and S3a). The average $\delta^{15}N$ value during warm months (−0.3‰) was close to that for the $\delta^{15}N$ lightning NO_x (Hoering, 1957), suggesting that the contribution of lightning NO_x increased during warm months. A global distribution map of lightning NO_x shows that maximum NO_x was produced from lightning during warm seasons in the SCS (Price et al., 1997). However, the maximum $\delta^{15}N$ value during the warm months (+4.8‰) suggests that NO_x may also originate from biomass burning (Hsu et al., 2014), since these emissions have possibly positive values (Hastings et al., 2003) and highest fire frequencies in northeast India and Southeast Asia countries occur during warm seasons (Hsu et al., 2014; Streets et al., 2003; Vadrevu et al., 2014). The minimum $\delta^{15}N$ value was −2.5‰ during the warm months, suggesting that NO_x in some events may also be derived from livestock or biogenic soil emissions in Southeast Asia (Fig. 2 and

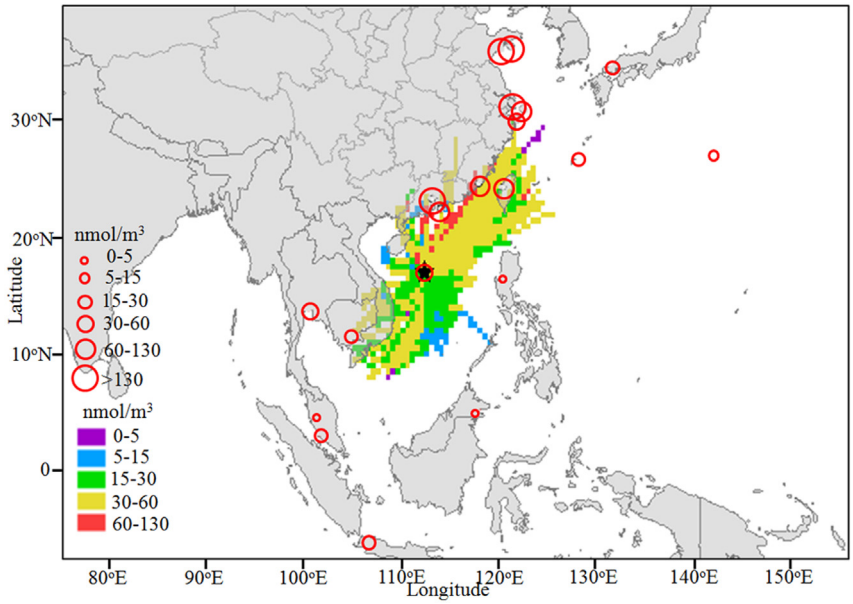

Fig. 1. Concentration weighted trajectory plots for NO_3^- at 36 h at Yongxing Island, the NO_3^- concentrations in EANET sites (http://www.eanet.asia/) and previous reported data NO_3^- concentrations in coast (Fang et al., 2002; Gao et al., 1996; Wang et al., 1992; Wang et al., 2006).

Fig. S1; Felix et al., 2012; Felix and Elliott, 2014; Li and Wang, 2008). So, the contribution of lightning NO_x is major with mix of other sources (biomass burning, livestock or biogenic soil emissions).

Interestingly, the concentrations and $\delta^{15}N$ values near the coast and on the Pearl River were much higher than those over open sea on the two NSCS cruises (Table S1); although we found that the average $\delta^{15}N$ values and NO_3^- concentrations on both Aug. and Nov. cruises were higher than those at Yongxing Island for the same period (Table 1). The differences in NO_3^- concentrations and $\delta^{15}N$ between NSCS and Yongxing Island suggest that NO_3^- or NO_x may be lost during air masses transport from polluted to remote regions, and ^{15}N was preferentially removed. A number of potential mechanisms could account for these changes.

One mechanism involves equilibrium fractionation between NO and NO_2, which depends on the NO_x and O_3 concentration in the atmosphere (R1 and R2) (Freyer et al., 1993). As nitrogen isotope exchange reactions take place, they result in ^{15}N enriched NO_2, when the ratio of NO_x concentration to O_3 concentration is higher than 1 (Fang et al., 2011; Freyer et al., 1993). However, the $\delta^{15}N$ of NO_2 would be equivalent to NO_x when the ratio of NO_x concentration to O_3 concentration is lower than 1, because in this case most of the NO is oxidized to NO_2 (Altieri et al., 2013; Freyer et al., 1993). O_3 concentrations always exceeded NO_x concentrations during cool months in the NSCS (Fig. S4), indicating that the $\delta^{15}N$ of NO_2 reflects $\delta^{15}N$ of sources. Although there are no data for NO_x and O_3 concentrations at Yongxing Island, much data have shown that O_3 concentrations exceed NO_x concentrations in remote marine atmospheres (Altieri et al., 2013; Ou-Yang et al., 2013). So, NO_x is mainly in the form of NO_2. This suggests that exchange reactions were not important in the source region and during the long-distance transmission to the Yongxing Island.

When atmospheric NO_x or N_yO_z occur over the ocean, they probably react with halogens (R9, R10, R12, and R17 in supplementary text). Such heterogeneous processes cause nitrogen isotopic fractionation and ^{15}N is preferentially incorporated into the more stable phase (Altieri et al., 2013). Overnight and in winter months, N_2O_5 potentially reacts with halides to form $ClNO_2$ and NO_3^-, because this pathway is significant in coastal marine atmospheres (Davidson and Kingerlee, 1997; Finlayson-Pitts, 2003; Keene et al., 1990; Knipping and Dabdub, 2003; Pechtl and von Glasow, 2007; Thornton et al., 2010). In this case, ^{15}N is preferentially incorporated into NO_3^-, leaving ^{14}N in gaseous $ClNO_2$ (Altieri et al., 2013). $ClNO_2$ reverts to NO_2 via photolysis at the day. Another possible mechanism involves the reaction of NO_2 and NaCl to form $NaNO_3$ and ClNO (R16), in which case, ^{15}N is also preferentially incorporated into $NaNO_3$. The life time of NO_3^- deposition is much shorter than NO_x. Therefore, the downwind concentration and $\delta^{15}N$ of NO_3^- is lower than for the source region. Since wind speed in cool seasons is higher than in warm seasons, more halides are likely released to the marine atmosphere in cool months (Lewandowska and Falkowska, 2013). In our study, the difference in $\delta^{15}N$ between the NSCS and Yongxing Island was +3.6‰ in Nov. 2013 (cool month).

4.3. Temporal and spatial variations in $\delta^{18}O$

The weighted average (by NO_3^- concentrations) $\delta^{18}O$ values for Aug. and Nov. from the NSCS (+65.6‰ and +71.8‰, respectively) are consistent with the $\delta^{18}O$ values in rainwater for summer and winter at Guangzhou (+63.5‰ in summer and +73.2‰ in winter; Fang et al., 2011), while the $\delta^{18}O$ values of NO_3^- in particles appear to reflect regions. They ranged from +53.1‰ to +111.4‰, with an average of +80.2‰ near Antarctica (Morin et al., 2009; Savarino et al., 2007), whereas Morin et al. (2009) reported $\delta^{18}O$ of NO_3^- in particles between +63.7‰ and +91.9‰, with an average of +74.6‰ above the Atlantic Ocean; these values are closest to our observed values. However, the average $\delta^{18}O$ values at Yongxing Island were much higher than at Dongsha Island (Yang et al., 2014) and our samples collected on two cruises in the NSCS. The weighted average (by NO_3^- concentrations) $\delta^{18}O$ value in TSP at Yongxing Island (+83.2‰) was only slightly higher than the average $\delta^{18}O$ value in rainwater at Guangzhou (+66.0‰) and Bermuda (+71.1‰) (Altieri et al., 2013; Fang et al., 2011).

As elsewhere, the $\delta^{18}O$ values exhibit seasonal variation, with higher values in cool months (Fig. 3a) and lower values in warm months (Fig. 3b), reflecting different oxidation pathways of NO_x to NO_3^- (Altieri et al., 2013; Fang et al., 2011). The different pathways are controlled by temperature, and solar radiation, and other

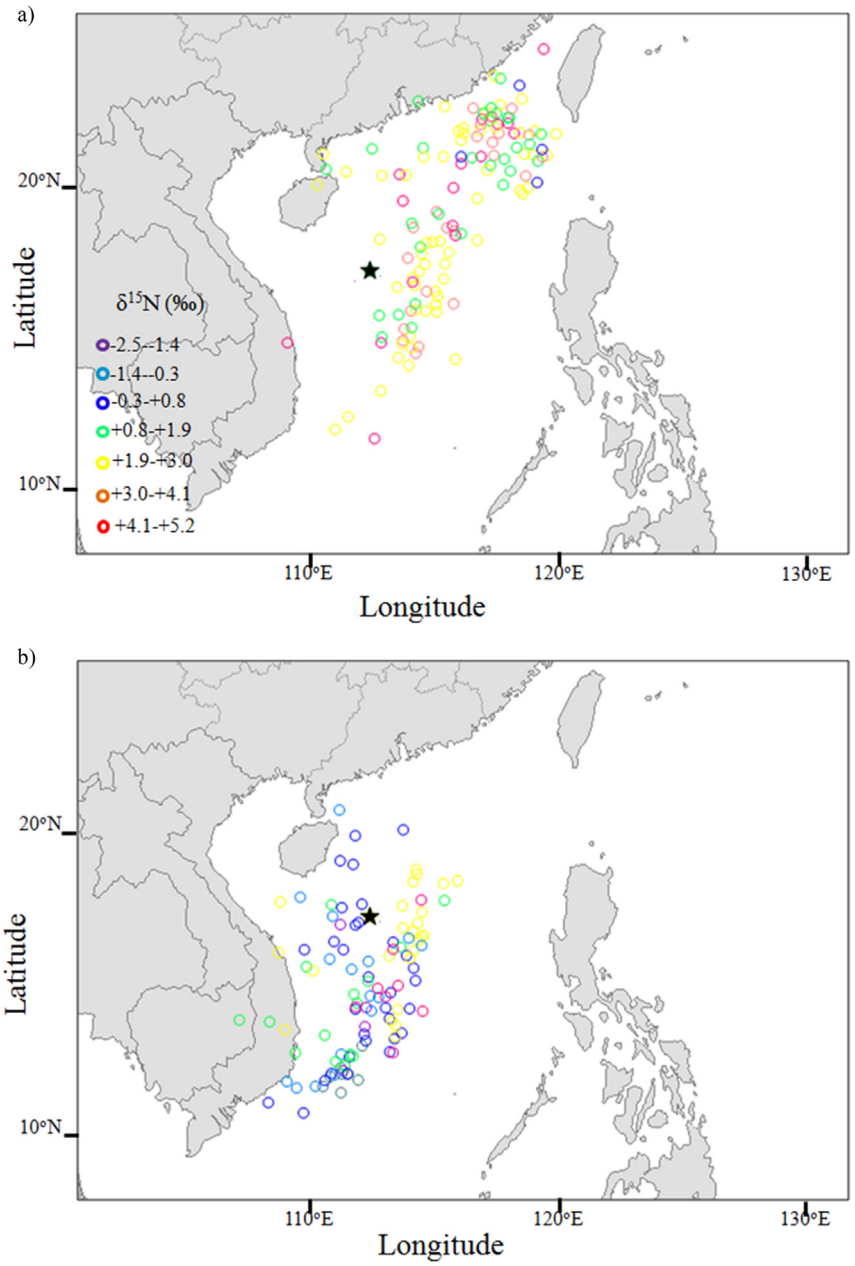

Fig. 2. $\delta^{15}N$ geographic distribution of TSP at 36 h before reaching Yongxing Island (a: cool season; b: warm season), based on NOAA HYSPLIT model air mass back trajectories.

meteorological conditions, in which N_2O_5 is thermally decomposed and OH is photolytically produced (Fang et al., 2011; Wankel et al., 2010). Generally, the oxygen atoms in NO_3^- are derived from 5/6O_3 and 1/6H_2O in the N_2O_5 pathway (R5 and R7) and from 2/3O_3 and 1/3OH radical in the OH radical pathway (R3) (Hastings et al., 2003). The $\delta^{18}O$ of O_3 has a relatively high value, within the range from +90‰ to +122‰; while the $\delta^{18}O$ of OH is close to water vapour in the troposphere, ranging from −15.0‰ to 0‰ in Asia Dubey et al., 1998; Fang et al., 2011; Johnston and Thiemens, 1997). Using the minimum and maximum values of $\delta^{18}O$ in O_3 and OH as estimates, then the $\delta^{18}O$ of NO_3^- should range from +55‰ to +102‰ (Fang et al., 2011). Most of our $\delta^{18}O$ values fell within this range. The longer daylight hours would increase OH concentration in the troposphere during warm months, but decreased daylight hours in cold months would enhance N_2O_5 hydrolysis. Therefore, seasonal variation in $\delta^{18}O$ values of NO_3^- could reflect seasonal variation in the chemical conversion of NO_x to NO_3^-. In our study, the weighted average (by NO_3^- concentrations) of $\delta^{18}O$ of NO_3^- was +71.2‰ during warm months and +88.9‰ during cool months. Higher $\delta^{18}O$ values were recorded from the northeast of SCS during cool months, while lower $\delta^{18}O$ values were recorded from the southwest during warm months. Furthermore, both the O_3 and OH concentrations have pronounced latitudinal gradients and seasonal variation that would amplify this pattern (Fishman et al., 1990; Spivakovsky et al., 2000; Weller et al., 1996).

During cooler hours at night or during winter, N_2O_5 reacts not only with H_2O, but also with HCl and NaCl to form NO_3^- in the marine atmosphere (R9 and R10). Given that the $\delta^{18}O$ of NO_3^- in the NSCS was much lower than at Yongxing Island (Table 1), we concluded that the $\delta^{18}O$ of NO_3^- increased because it was not diluted by oxygen atoms from water and/or OH. In addition to the OH and N_2O_5 oxidation pathways, halogen also provides a pathway (R15

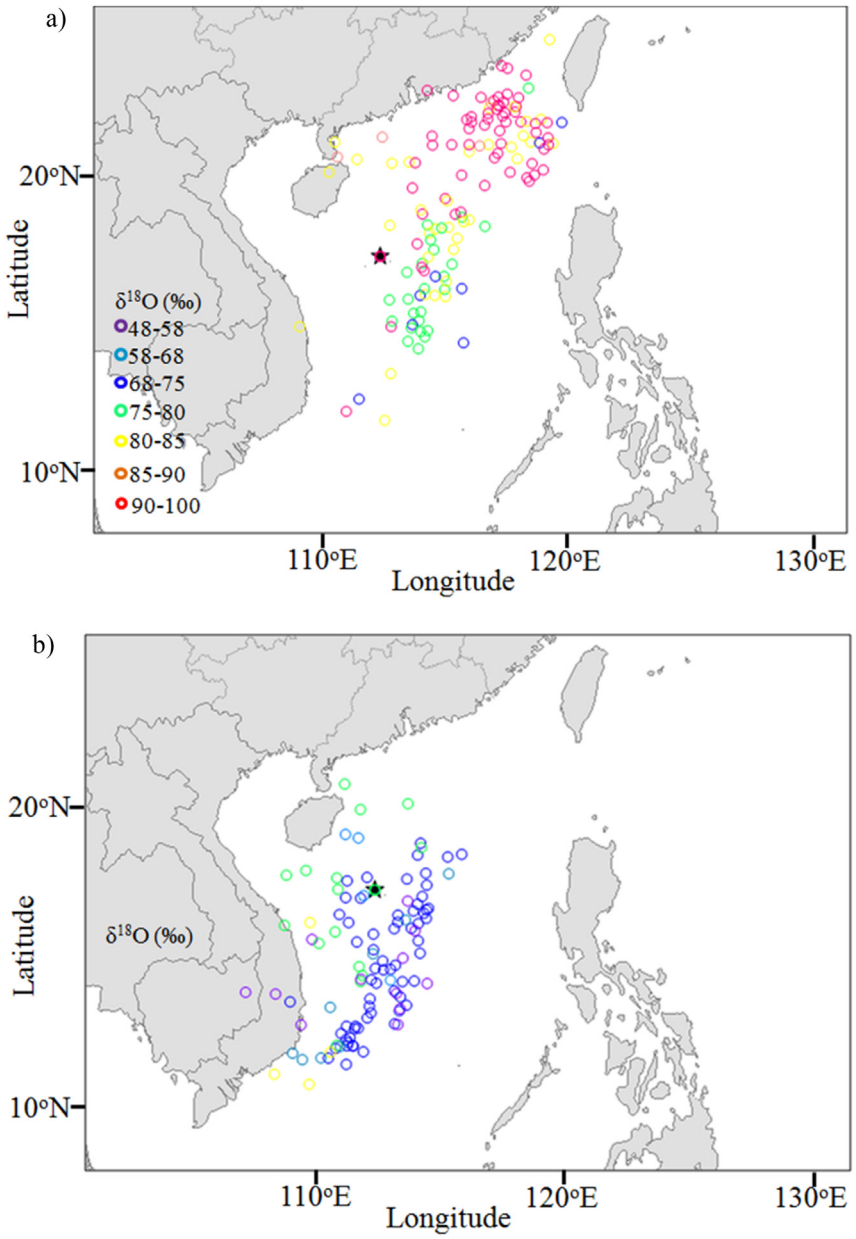

Fig. 3. $\delta^{18}O$ geographic distribution of TSP at 36 h before reaching Yongxing Island (a: cool season; b: warm season), based on NOAA HYSPLIT model air mass back trajectories.

and R16). Cl is produced in the reactions R10 and R18, and allowing it to react with O_3 to form ClO (R13). NO_2 reacts with ClO (R15) to form $ClNO_3$, and then $ClNO_3$ reacts with NaCl (R16) to from $NaNO_3$. The oxygen atom in ClO is obtained from O_3, so the $\delta^{18}O$ of $NaNO_3$ formed from $ClNO_3$ is high. The $ClNO_2$ concentration in R10, and ClNO concentration in R17 are highest, when sea salt concentration and O_3 concentration are highest during cool seasons (Njegic et al., 2010; Osthoff et al., 2008). This suggests that there is an influence from heterogeneous halogen chemistry on the $\delta^{18}O$ of NO_3^- in the cool season (Altieri et al., 2013).

4.4. Relationship between $\delta^{15}N$ and $\delta^{18}O$ of NO_3^-

Previous studies found a negative linear correlation between $\delta^{15}N$ and $\delta^{18}O$ values of NO_3^- in marine atmospheric environments, suggesting that atmospheric chemical processes and variations in nitrogen sources influence nitrogen and oxygen isotopic composition (Altieri et al., 2013; Hastings et al., 2003; Yang et al., 2014). Terrestrial studies suggested there was a positive linear correlation between them (Elliott et al., 2009). We found a positive linear relationship between $\delta^{15}N$ and $\delta^{18}O$ values of NO_3^- in all TSP samples ($R = 0.26$, $P = 0.047$) at Yongxing Island (Fig. 4). A positive linear relationship was also found in transition months (Apr. or Aug.) at Yongxing Island ($R = 0.62$, $P = 0.03$) and in the NSCS in Aug. ($R = 0.79$, $P = 0.02$; Fig. 4). In those months, the $\delta^{15}N$ and $\delta^{18}O$ values in NO_3^- were controlled by sources with different nitrogen isotope composition and different oxidation pathway. In cool months, high $\delta^{15}N$ was associated with high $\delta^{18}O$ at Yongxing Island because of the influx of high concentrations of NO_x with high $\delta^{15}N$ values from Chinese coastal cities, and the increased role of O_3 with lower temperature and longer nights (Altieri et al., 2013). In warm months, the O_3 signal was diluted by the increased participation of OH and H_2O in the formation of nitrate, resulting in an overall lower $\delta^{18}O$. The increased contribution from lighting, and biogenic soil

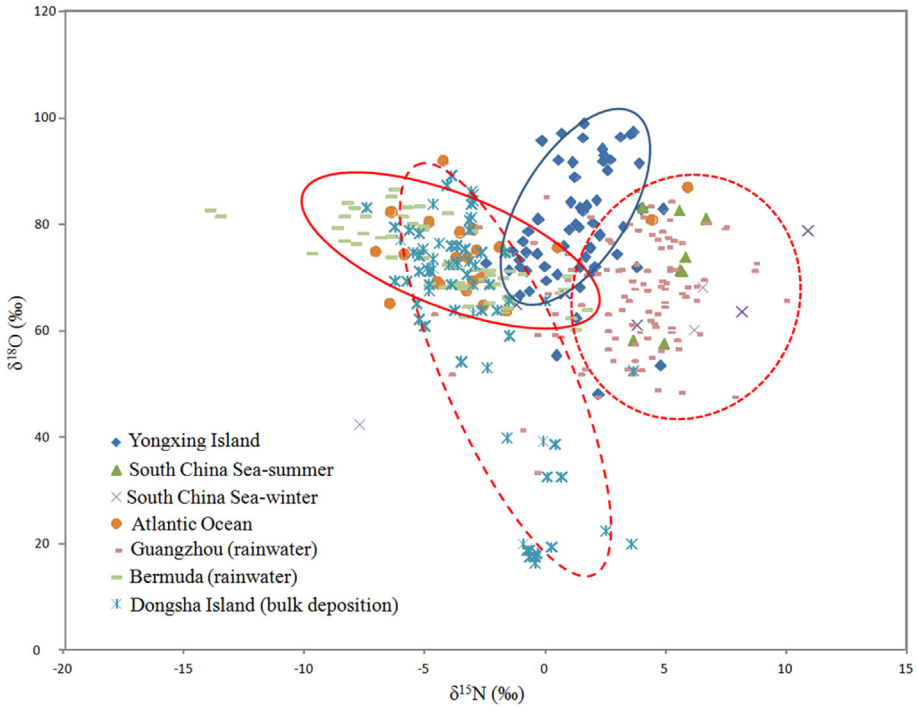

Fig. 4. The relationship between $\delta^{15}N$ and $\delta^{18}O$ in TSP at Yongxiang Island, in TSP in Northern South China Sea, in rainwater at Guangzhou (Fang et al., 2011), in bulk deposition at Dongsha Island (Yang et al., 2014), in rainwater at Bermuda (Altieri et al., 2013) and in aerosol in Atlantic Ocean (Morin et al., 2009). For all samples at Yongxing Island, $R = 0.26$, $P = 0.047$; for transition season at Yongxing Island, $R = 0.62$, $P = 0.03$. For samples in warm months in NSCS, $R = 0.79$, $P = 0.02$; for samples in cool months in NSCS, $R = 0.42$, $P > 0.05$.

contributed to lower $\delta^{15}N$ values. Although the negative linear relationship was found at Dongsha Island (Yang et al., 2014), this may reflect the unusually low $\delta^{18}O$ in summer. No relationship between $\delta^{15}N$ and $\delta^{18}O$ was found at Yongxing Island, the NSCS or at Dongsha Island (Yang et al., 2014) in cool months ($P > 0.05$), suggesting that complex sources of NO_x and high concentrations of O_3 influence this relationship.

We found lower $\delta^{15}N$ and higher $\delta^{18}O$ in TSP at Yongxing Island compared with TSP and rainwater samples from South China coastal areas (Fig. 4). This suggests that $\delta^{15}N$ decreased and $\delta^{18}O$ increased during transport from coastal to remote sea setting. If the source of the NO_3^- deposited in Yongxing Island during the cool months is the same as that deposited in the South China coastal areas, then the pool of NO_x and its oxidation products must preferentially lose ^{15}N and have a high $\delta^{18}O$. If the NO_3^- in the coarse mode derived all its oxygen atoms from O_3 (R12-R15) (Gobel et al., 2013), the $\delta^{18}O$ of NO_3^- formed in the coastal areas should not be changed during transport to Yongxing Island. However, the $\delta^{18}O$ of NO_3^- formed during transport did increase. To explore this, we assumed that during the cool months, the oxygen atoms in NO_3^- formed by NO_x are derived from O_3 and oxygen atoms of NO_3^- from coastal NO_3^- (formed before transport) did not change during transport or deposition from the coast to Yongxing Island. Thus,

$$\delta^{18}O - NO_3^-(TSP) = \delta^{18}O - NO_3^-(NOx) \times Z + \delta^{18}O - NO_3^-(coast) \times (1 - Z) \quad (1)$$

where Z is the ratio of NO_3^- formed by NO_x to the total NO_3^- of TSP.

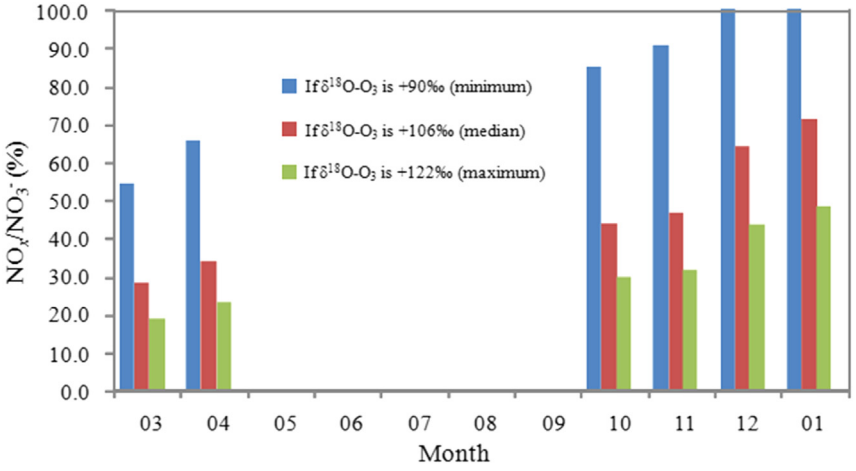

Fig. 5. The ratios of NO_3^- formed by NO_x to total NO_3^- of TSP at Yongxing Island in different cool months.

The $\delta^{18}O$ of coastal NO_3^- is +73‰, which is equivalent to the mean $\delta^{18}O$ value of TSP from NSCS in Nov. (this study) and winter rainwater samples from Guangzhou (Fang et al., 2011). Thus, the ratio of NO_3^- formed by NO_x to total NO_3^- can be calculated for cool months at Yongxing Island (Fig. 5). Given the wide range of $\delta^{18}O$ of O_3 (+90‰-+122‰), the minimum (+90‰), maximum (+122‰), and median (+106‰) values were used to calculate this ratios, yielding values of 82.5%, 32.2% and 47.9%, respectively. In the open sea, the molar ratio of NO_3^- to NO_x was relative high (>10 at Hedo Island; http://www.eanet.asia/). If we ignore the NO_x concentration at Yongxing Island and use the synchronous observations in Nov. 2013 between Yongxing Island and the Chinese coast (130.6 nmol/m^3, NO_3^- data from our observations, and 188.4 nmol/m^3, NO_x data from www.epd.gov.hk), then NO_3^- from NO_x is calculated to be 17.6 nmol/m^3 and the coastal NO_3^- was 19.9 nmol/m^3 (formed before transport), using a median ratio for NO_3^- formed by NO_x to total NO_3^- of TSP of 46.5%. Hence, 87% of NO_3^- and 89% of NO_x were lost during the transport from coast to Yongxing Island; although inclusion of other chemical pathways involving conversion of NO_x to NO_3^-, dry and wet NO_x deposition during transport must be evaluated to obtain exact loss ratios.

5. Conclusions

Average NO_3^- concentrations, and $\delta^{15}N$ and $\delta^{18}O$ values for NO_3^- in TSP at Yongxing Island over the yearlong study period were 34.9 nmol/m^3, +1.5‰ and +83.2‰, respectively. Values of $\delta^{15}N$ and $\delta^{18}O$ in TSP showed spatial and seasonal variations, indicating that they had different sources and chemical pathways for different seasons. In cool months, NO_3^- with higher concentrations, and $\delta^{15}N$ and $\delta^{18}O$ values indicated that origins were from northeast of Yongxing Island, from anthropogenic sources in South China with high nitrogen deposition. In warm months, the contribution of natural emissions was more important. There was a decrease in $\delta^{15}N$ and increase $\delta^{18}O$ during transport from coast of South China to Yongxing Island during cool months, because ^{15}N is preferentially lost and oxygen atoms were mainly from O_3 during transport.

Acknowledgements

This work was supported by the National Natural Science Foundation of China through Grants 41203015 (H.-W. Xiao), 41273027, 41173027 (H.-Y. Xiao), and 40721002 (C.-Q. Liu), as well as the Strategic Priority Research Program of the Chinese Academy of Sciences through Grants XDA11030103 and XDA11020202 (A.M. Long).

Appendix A. Supplementary data

Supplementary data related to this article can be found at http://dx.doi.org/10.1016/j.atmosenv.2015.03.006.

References

Altieri, K.E., Hastings, M.G., Gobel, A.R., Peters, A.J., Sigman, D.M., 2013. Isotopic composition of rainwater nitrate at Bermuda: the influence of air mass source and chemistry in the marine boundary layer. J. Geophys. Res. Atmos. 118 (19), 11, 304–311, 316.

Ammann, M., Siegwolf, R., Pichlmayer, F., Suter, M., Saurer, M., Brunold, C., 1999. Estimating the uptake of traffic-derived NO_2 from 15N abundance in Norway spruce needles. Oecologia 118 (2), 124–131.

Calvert, J.G., Lazrus, A., Kok, G.L., Heikes, B.G., Walega, J.G., Lind, J., Cantrell, C.A., 1985. Chemical mechanisms of acid generation in the troposphere. Nature 317, 27–35.

Chameides, W.L., 1984. The photochemistry of a remote marine stratiform cloud. J. Geophys. Res. Atmos. 89 (D3), 4739–4755 (1984–2012).

Davidson, E.A., Kingerlee, W., 1997. A global inventory of nitric oxide emissions from soils. Nutrient Cycl. Agroecosyst. 48 (1–2), 37–50.

Dubey, M.K., Mohrschladt, R., Donahue, N.M., Anderson, J.G., 1998. Isotope specific kinetics of hydroxyl radical (OH) with water (H_2O): testing models of reactivity and atmospheric fractionation. J. Phys. Chem. A 101 (8), 1494–1500.

Duce, R.A., LaRoche, J., Altieri, K., Arrigo, K.R., Baker, A.R., Capone, D.G., Cornell, S., Dentener, F., Galloway, J., Ganeshram, R.S., 2008. Impacts of atmospheric anthropogenic nitrogen on the open ocean. Science 320 (5878), 893–897.

Elliott, E.M., Kendall, C., Boyer, E.W., Burns, D.A., Lear, G.G., Golden, H.E., Harlin, K., Bytnerowicz, A., Butler, T.J., Glatz, R., 2009. Dual nitrate isotopes in dry deposition: utility for partitioning NO_x source contributions to landscape nitrogen deposition. J. Geophys. Res. Biogeosciences 114 (G4). http://dx.doi.org/10.1029/2008JG000889 (2005–2012).

Falkowski, P.G., Barber, R.T., Smetacek, V., 1998. Biogeochemical controls and feedbacks on ocean primary production. Science 281 (5374), 200–206.

Fang, G., Chang, C., Wu, Y., Fu, P.P., Yang, C., Chen, C., Chang, S., 2002. Ambient suspended particulate matters and related chemical species study in central Taiwan, Taichung during 1998–2001. Atmos. Environ. 36 (12), 1921–1928.

Fang, Y.T., Koba, K., Wang, X.M., Wen, D.Z., Li, J., Takebayashi, Y., Liu, X.Y., Yoh, M., 2011. Anthropogenic imprints on nitrogen and oxygen isotopic composition of precipitation nitrate in a nitrogen-polluted city in southern China. Atmos. Chem. Phys. 11 (3), 1313–1325.

Felix, J.D., Elliott, E.M., 2014. Isotopic composition of passively collected nitrogen dioxide emissions: vehicle, soil and livestock source signatures. Atmos. Environ. 92, 359–366.

Felix, J.D., Elliott, E.M., Shaw, S.L., 2012. Nitrogen isotopic composition of coal-fired power plant NO_x: influence of emission controls and implications for global emission inventories. Environ. Sci. Technol. 46 (6), 3528–3535.

Fibiger, D.L., Hastings, M.G., Lew, A.F., Peltier, R.E., 2014. Collection of NO and NO_2 for isotopic Analysis of NO_x Emissions. Anal. Chem. 86, 12115–12121.

Finlayson-Pitts, B.J., 2003. The tropospheric chemistry of sea salt: a molecular-level view of the chemistry of NaCl and NaBr. Chem. Rev. 103 (12), 4801–4822.

Finlayson-Pitts, B.J., Pitts Jr., J.N., 1999. Chemistry of the Upper and Lower Atmosphere: Theory, Experiments, and Applications. Academic Press.

Fishman, J., Watson, C.E., Larsen, J.C., Logan, J.A., 1990. Distribution of tropospheric ozone determined from satellite data. J. Geophys. Res. Atmos. 95 (D4), 3599–3617 (1984–2012).

Freyer, H.D., Kley, D., Volz Thomas, A., Kobel, K., 1993. On the interaction of isotopic exchange processes with photochemical reactions in atmospheric oxides of nitrogen. J. Geophys. Res. Atmos. 98 (D8), 14791–14796 (1984–2012).

Freyer, H.D., Kobel, K., Delmas, R.J., Kley, D., Legrand, M.R., 1996. First results of $^{15}N/^{14}N$ ratios in nitrate from alpine and polar ice cores. Tellus Ser. B-Chemical Phys. Meteorology 48 (1), 93–105.

Galloway, J.N., Townsend, A.R., Erisman, J.W., Bekunda, M., Cai, Z., Freney, J.R., Martinelli, L.A., Seitzinger, S.P., Sutton, M.A., 2008. Transformation of the nitrogen cycle: recent trends, questions, and potential solutions. Science 320 (5878), 889–892.

Gao, J., 1996. Preliminary study on the aerosol characteristics of Xiamen in spring. Environ. Sci. 9, 33–37 (in Chinese with English abstract).

Gobel, A.R., Altieri, K.E., Peters, A.J., Hastings, M.G., Sigman, D.M., 2013. Insights into anthropogenic nitrogen deposition to the North Atlantic investigated using the isotopic composition of aerosol and rainwater nitrate. Geophys. Res. Lett. 40 (22), 5977–5982.

Hastings, M.G., Jarvis, J.C., Steig, E.J., 2009. Anthropogenic impacts on nitrogen isotopes of ice-core nitrate. Science 324 (5932), 1288.

Hastings, M.G., Sigman, D.M., Lipschultz, F., 2003. Isotopic evidence for source changes of nitrate in rain at Bermuda. J. Geophys. Res. Atmos. 108 (D24) http://dx.doi.org/10.1029/2003JD003789 (1984–2012).

Heaton, T., 1987. $^{15}N/^{14}N$ ratios of nitrate and ammonium in rain at Pretoria, South Africa. Atmos. Environ. 21 (4), 843–852 (1967).

Heaton, T., 1990. $^{15}N/^{14}N$ ratios of NO_x from vehicle engines and coal-fired power stations. Tellus Ser. B-Chemical and Phys. Meteorology 42 (3), 304–307.

Heaton, T.H., Wynn, P., Tye, A.M., 2004. Low $^{15}N/^{14}N$ ratios for nitrate in snow in the high Arctic (79° N). Atmos. Environ. 38 (33), 5611–5621.

Hoering, T., 1957. The isotopic composition of the ammonia and the nitrate ion in rain. Geochimica Cosmochimica Acta 12 (1), 97–102.

Hsu, S.C., Gong, G.C., Shiah, F.K., Hung, C.C., Kao, S.J., Zhang, R., Chen, W.N., Chen, C.C., Chou, C.C.K., Lin, Y.C., Lin, F.J., Lin, S.H., 2014. Sources, solubility, and acid processing of aerosol iron and phosphorous over the South China Sea: east Asian dust and pollution outflows vs. Southeast Asian biomass burning. Atmos. Chemsitry Phys. Discuss. 14, 21433–21472.

Johnston, J.C., Thiemens, M.H., 1997. The isotopic composition of tropospheric ozone in two environments. J. Geophys. Res. Atmos. 102 (D21), 25395–25404 (1984–2012).

Keene, W.C., Pszenny, A.A., Jacob, D.J., Duce, R.A., Galloway, J.N., Schultz Tokos, J.J., Sievering, H., Boatman, J.F., 1990. The geochemical cycling of reactive chlorine through the marine troposphere. Glob. Biogeochem. Cycles 4 (4), 407–430.

Kendall, C., 1998. Tracing nitrogen sources and cycling in catchments. In: Kendall, C., McDonnell, J.J. (Eds.), Isotope Tracers in Catchment Hydrology. Elsevier, Amsterdam, pp. 519–576.

Kiga, T., Watanabe, S., Yoshikawa, K., Asano, K., Okitsu, S., Tsunogai, U., Narukawa, K., 2000. Evaluation of NOx formation in pulverized coal firing by use of nitrogen isotope ratios. In: International Joint Power Generation Conference 2000.

Kim, T.W., Lee, K., Duce, R., Liss, P., 2014. Impact of atmospheric nitrogen deposition on phytoplankton productivity in the South China Sea. Geophys. Res. Lett. 41 (9), 3156–3162.

Knipping, E.M., Dabdub, D., 2003. Impact of chlorine emissions from sea-salt aerosol

on coastal urban ozone. Environ. Sci. Technol. 37 (2), 275–284.
Krankowsky, D., Bartecki, F., Klees, G.G., Mauersberger, K., Schellenbach, K., Stehr, J., 1995. Measurement of heavy isotope enrichment in tropospheric ozone. Geophys. Res. Lett. 22 (13), 1713–1716.
Lewandowska, A.U., Falkowska, L.M., 2013. Sea salt in aerosols over the southern Baltic. Part 1. The generation and transportation of marine particles. Oceanologia 55 (2), 279–298.
Li, D., Wang, X., 2008. Nitrogen isotopic signature of soil-released nitric oxide (NO) after fertilizer application. Atmos. Environ. 42 (19), 4747–4754.
McIlvin, M.R., Altabet, M.A., 2005. Chemical conversion of nitrate and nitrite to nitrous oxide for nitrogen and oxygen isotopic analysis in freshwater and seawater. Anal. Chem. 77 (17), 5589–5595.
Moore, H., 1977. The isotopic composition of ammonia, nitrogen dioxide and nitrate in the atmosphere. Atmos. Environ. 11 (12), 1239–1243 (1967).
Morin, S., Savarino, J., Frey, M.M., Domine, F., Jacobi, H.W., Kaleschke, L., Martins, J.M., 2009. Comprehensive isotopic composition of atmospheric nitrate in the Atlantic ocean boundary layer from 65°S to 79°N. J. Geophys. Res. Atmos. 114 (D5) http://dx.doi.org/10.1029/2008JD010696 (1984–2012).
Morin, S., Savarino, J., Frey, M.M., Yan, N., Bekki, S., Bottenheim, J.W., Martins, J.M., 2008. Tracing the origin and fate of NO_x in the Arctic atmosphere using stable isotopes in nitrate. Science 322 (5902), 730–732.
Njegic, B., Raff, J.D., Finlayson-Pitts, B.J., Gordon, M.S., Gerber, R.B., 2010. Catalytic role for water in the atmospheric production of ClNO. J. Phys. Chem. A 114 (13), 4609–4618.
Olivier, J., Bouwman, A.F., Van der Hoek, K.W., Berdowski, J., 1998. Global air emission inventories for anthropogenic sources of NO_x, NH_3 and N_2O in 1990. Environ. Pollut. 102 (1), 135–148.
Osthoff, H.D., Roberts, J.M., Ravishankara, A.R., Williams, E.J., Lerner, B.M., Sommariva, R., Bates, T.S., Coffman, D., Quinn, P.K., Dibb, J.E., 2008. High levels of nitryl chloride in the polluted subtropical marine boundary layer. Nat. Geosci. 1 (5), 324–328.
Ou-Yang, C., Hsieh, H., Wang, S., Lin, N., Lee, C., Sheu, G., Wang, J., 2013. Influence of Asian continental outflow on the regional background ozone level in Northern South China Sea. Atmos. Environ. 78, 144–153.
Pechtl, S., von Glasow, R., 2007. Reactive chlorine in the marine boundary layer in the outflow of polluted continental air: a model study. Geophys. Res. Lett. 34 (11) http://dx.doi.org/10.1029/2007GL029761.
Price, C., Penner, J., Prather, M., 1997. NO_x from lightning: 1. Global distribution based on lightning physics. J. Geophys. Res. Atmos. 102 (D5), 5929–5941 (1984–2012).
Ryabenko, E., Altabet, M.A., Wallace, D.W., 2009. Effect of chloride on the chemical conversion of nitrate to nitrous oxide for $\delta^{15}N$ analysis. Limnol. Oceanogr. Methods 7, 545–552.
Savarino, J., Kaiser, J., Morin, S., Sigman, D.M., Thiemens, M.H., 2007. Nitrogen and oxygen isotopic constraints on the origin of atmospheric nitrate in coastal Antarctica. Atmos. Chem. Phys. 7 (8), 1925–1945.
Schumann, U., Huntrieser, H., 2007. The global lightning-induced nitrogen oxides source. Atmos. Chem. Phys. 7 (14), 3823–3907.
Seinfeld, J.H., Pandis, S.N., 2012. Atmospheric Chemistry and Physics: from Air Pollution to Climate Change. John Wiley & Sons.
Spivakovsky, C.M., Logan, J.A., Montzka, S.A., Balkanski, Y.J., Foreman Fowler, M., Jones, D., Horowitz, L.W., Fusco, A.C., Brenninkmeijer, C., Prather, M.J., 2000. Two-dimensional climatological distribution of tropospheric OH: update and evaluation. J. Geophys. Res. Atmos. 105 (D7), 8931–8980 (1984–2012).
Streets, D.G., Yarber, K.F., Woo, J.H., Carmichael, G.R., 2003. Biomass burning in Asia: annual and seasonal estimates and atmospheric emissions. Glob. Biogeochem. Cycles 17 (4). http://dx.doi.org/10.1029/2003GB002040.
Thornton, J.A., Kercher, J.P., Riedel, T.P., Wagner, N.L., Cozic, J., Holloway, J.S., Dubé, W.P., Wolfe, G.M., Quinn, P.K., Middlebrook, A.M., 2010. A large atomic chlorine source inferred from mid-continental reactive nitrogen chemistry. Nature 464 (7286), 271–274.
Tian, H.Z., Hao, J.M., Lu, Y.Q., Zhu, T.L., 2001. Inventories and distribution characteristics of NOx emissions in China. China Environ. Sci. 21 (6), 493–497 (in Chinese with English abstract).
Vadrevu, K.P., Lasko, K., Justice, C., 2014. Spatial variations in vegetation fires and carbon monoxide concentrations in south Asia. In: Remote Sensing Applications in Environmental Research. Springer, pp. 131–149.
Wang, W., Jiang, Z., Zhang, M., Wang, W., 1992. Pollution characteristic of atmospheric aerosol and relationship between aerosol and acid precipitation in South China. Acta Sci. Circumstantiae 12, 8–15 (in Chinese with English abstract).
Wang, Y., Zhuang, G., Zhang, X., Huang, K., Xu, C., Tang, A., Chen, J., An, Z., 2006. The ion chemistry, seasonal cycle, and sources of $PM^{2.5}$ and TSP aerosol in Shanghai. Atmos. Environ. 40 (16), 2935–2952.
Wang, Y.Q., Zhang, X.Y., Draxler, R.R., 2009. TrajStat: GIS-based software that uses various trajectory statistical analysis methods to identify potential sources from long-term air pollution measurement data. Environ. Model. Softw. 24 (8), 938–939.
Wankel, S.D., Chen, Y., Kendall, C., Post, A.F., Paytan, A., 2010. Sources of aerosol nitrate to the gulf of Aqaba: evidence from $\delta^{15}N$ and $\delta^{18}O$ of nitrate and trace metal chemistry. Mar. Chem. 120 (1), 90–99.
Weller, R., Lilischkis, R., Schrems, O., Neuber, R., Wessel, S., 1996. Vertical ozone distribution in the marine atmosphere over the central Atlantic ocean (56°S–50°N). J. Geophys. Res. Atmos. 101 (D1), 1387–1399 (1984–2012).
Xiao, H., Liu, C., 2002. Sources of nitrogen and sulfur in wet deposition at Guiyang, southwest China. Atmos. Environ. 36 (33), 5121–5130.
Xiao, H.W., Xiao, H.Y., Long, A.M., Wang, Y.L., 2012. Nitrogen isotopic composition and source of nitrate in precipitation at Guiyang. Acta Sci. Circumstantiae 32 (4), 940–945 (in Chinese with English abstract).
Yang, J., Hsu, S., Dai, M., Hsiao, S., Kao, S., 2014. Isotopic composition of water-soluble nitrate in bulk atmospheric deposition at Dongsha Island: sources and implications of external N supply to the northern South China Sea. Biogeosciences 11, 1833–1846.
Zhang, Q., Streets, D.G., He, K., Wang, Y., Richter, A., Burrows, J.P., Uno, I., Jang, C.J., Chen, D., Yao, Z., 2007. NO_x emission trends for China, 1995–2004: the view from the ground and the view from space. J. Geophys. Res. Atmos. 112 (D22) http://dx.doi.org/10.1029/2007JD008684 (1984–2012).
Zheng, J.Y., Zhang, L.J., Zhong, L.J., Wang, Z.L., 2009. Area source emission inventory of air pollutant and its spatial distribution characteristics in Pearl River Delta. China Environ. Sci. 29, 455–460 (in Chinese with English abstract).